

## Floquet-Rydberg quantum simulator for confinement in $\mathbb{Z}_2$ gauge theories

Enrico C. Domanti,<sup>1,2,3,\*</sup> Dario Zappalà<sup>3,4</sup>, Alejandro Bermudez,<sup>5,†</sup> and Luigi Amico<sup>1,2,3,6</sup>

<sup>1</sup>Quantum Research Centre, Technology Innovation Institute, 9639 Abu Dhabi, UAE

<sup>2</sup>Dipartimento di Fisica e Astronomia, Università di Catania, Via S. Sofia 64, 95123 Catania, Italy

<sup>3</sup>INFN-Sezione di Catania, Via S. Sofia 64, 95123 Catania, Italy

<sup>4</sup>Centro Siciliano di Fisica Nucleare e Struttura della Materia, Via S. Sofia 64, 95123 Catania, Italy

<sup>5</sup>Instituto de Física Teórica, UAM-CSIC, Universidad Autónoma de Madrid, Cantoblanco, 28049 Madrid, Spain

<sup>6</sup>Centre for Quantum Technologies, National University of Singapore, 3 Science Drive 2, Singapore 117543, Singapore



(Received 29 December 2023; accepted 5 April 2024; published 11 June 2024)

Recent advances in the field of quantum technologies have opened up the road for the realization of small-scale quantum simulators of lattice gauge theories which, among other goals, aim at improving our understanding on the nonperturbative mechanisms underlying the confinement of quarks. In this work, considering periodically driven arrays of Rydberg atoms in a tweezer ladder geometry, we devise a scalable Floquet scheme for the quantum simulation of the real-time dynamics in a  $\mathbb{Z}_2$  LGT, in which hardcore bosons/spinless fermions are coupled to dynamical gauge fields. Resorting to an external magnetic field to tune the angular dependence of the Rydberg dipolar interactions, and by a suitable tuning of the driving parameters, we manage to suppress the main gauge-violating terms and show that an observation of gauge-invariant confinement dynamics in the Floquet-Rydberg setup is at reach of current experimental techniques. Depending on the lattice size, we present a thorough numerical test of the validity of this scheme using either exact diagonalization or matrix-product-state algorithms for the periodically modulated real-time dynamics.

DOI: [10.1103/PhysRevResearch.6.L022059](https://doi.org/10.1103/PhysRevResearch.6.L022059)

*Introduction.* Gauge theory provides us with the basic language to understand the fundamental interactions [1]. Such theories arise from promoting global symmetries, e.g.,  $SU(3)$  [ $SU(2)_L \times U(1)$ ] for the strong (electroweak) interactions, to local ones by the introduction of gauge fields coupled to matter [2]. The discretization of gauge theories on a space-time lattice not only provides a natural cutoff, but a means to go beyond perturbative calculations [3], which is crucial to understand phenomena such as quark confinement [4]. In spite of the enormous progress of imaginary-time Monte Carlo methods for lattice gauge theories (LGTs), epitomized by the verification of the quark-model prediction of the hadron masses [5], finite-density and real-time phenomena are still beyond reach [6]. An approach to overcome these limitations arises from realizing that the lattice is not compelled to be a mathematical construct, but may indeed have a physical reality. Recent advances in quantum technology provide an effective avenue to implement the above program. By a careful experimental design, one can tailor the lattice and control the real-time matter dynamics to mimic the target model, thus

realizing a LGT quantum simulator (QS) [7,8]. These Qs can be thought of as special-purpose quantum computers [9], and their use for LGTs has recently raised the interest of a broad and diverse community (see the recent reviews [10–17]).

In spite of recent experimental progress [10–17], current technologies are still far from allowing large-scale Qs of the standard model of particle physics. This limitation is either due to the accumulation of errors for Qs operating in digital mode, or to the limited flexibility of Qs operating in the analog mode. To exploit the full potential of analog Qs, which are in principle more amenable for scaling in the presence of errors [18,19], it is of primary importance to devise novel schemes that engineer the high-weight terms characteristic of gauge theories in timescales that are faster than current decoherence sources. To devise these fundamental schemes as building blocks of more complicated models, the community is focusing on models in reduced spacetime dimensions and simpler gauge groups [20–24], which can still provide important insights. The  $\mathbb{Z}_2$  LGT is a paradigmatic case in this regard [24]. On one hand, it is a playground to understand confinement (deconfinement) in (1+1) dimensional chains [25,26] (ladders [27,28]). At the same time, the  $\mathbb{Z}_2$  LGT in 2+1 dimensions serves to understand central questions in condensed matter as topological order [29,30], confined and Higgs phases [31,32], and the interplay of superconductivity and charge deconfinement [33,34]. In the context of Qs, targeting these simpler LGTs dispenses with additional complications in higher dimensions and non-Abelian gauge groups. Although LGTs can sometimes be simulated effectively, e.g., integrating the gauge fields [35,36] or vice versa

\*Enrico.Domanti@tii.ae

†On sabbatical at Department of Physics, University of Oxford, Clarendon Laboratory, Parks Road, Oxford, UK.

Published by the American Physical Society under the terms of the Creative Commons Attribution 4.0 International license. Further distribution of this work must maintain attribution to the author(s) and the published article's title, journal citation, and DOI.

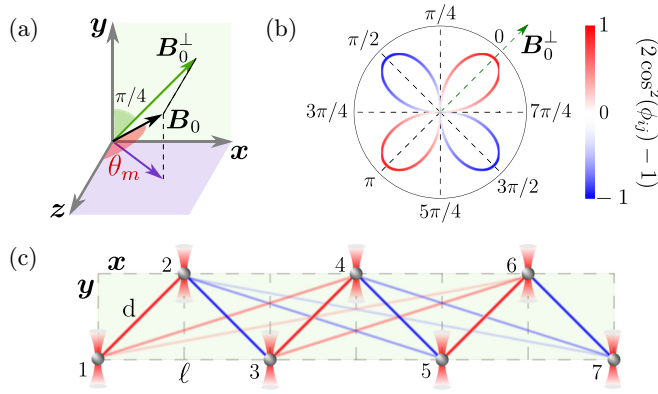


FIG. 1. *Rydberg tweezer array.* (a) The external magnetic field  $\mathbf{B}_0$  makes an angle  $\theta_m = 54.7^\circ$  with respect to the  $z$  axis. The projection of  $\mathbf{B}_0$  onto the  $xy$  plane where the atoms reside,  $\mathbf{B}_0^\perp$ , makes an angle of  $45^\circ$  with the  $x$  axis. (b) Angular distribution of the XY couplings as a function of the angle  $\phi_{ij}$  between the interatomic vector  $\mathbf{R}_{ij}$  and  $\mathbf{B}_0^\perp$ , which vanish at the critical angles  $\phi_{ij} = \pm 45^\circ, \pm 135^\circ$ . (c) Ladder configuration of the Rydberg atoms trapped in optical tweezers. The atoms are arranged on the vertices of isosceles right triangles of sides  $d$  and base  $b = \sqrt{2}d$ . The interactions are represented as colored lines according to the color scheme of panel (b). Dashed lines highlight the critical directions of the vanishing XY terms, which forbid a direct coupling between even-even and odd-odd spins. In this paper, we drive the odd atoms detuning according to  $H_{\text{drive}} = \sum_{i \text{ odd}} \frac{\eta \omega_d}{2} \cos(\omega_d t + \varphi_i) \sigma_i^z$ , with  $\eta \approx 2.4$  and  $\phi_{2i+1} = i\frac{\pi}{2}$ .

[37,38], developing schemes where matter and gauge fields correspond to physical degrees of freedom of the QS is essential to observe their interplay in confinement, as emphasized in recent proposals based on neutral atoms [39] and trapped ions [40]. Although these proposals can be, in principle, scaled up [41–48], so far, experiments have demonstrated only building blocks of the full theory [49,50].

In this work, we provide a scalable analog QS for the  $\mathbb{Z}_2$  LGT based on Rydberg atoms in optical tweezers [51,52]. We shall focus on a scheme which encodes a spin-1/2 variable in a pair of nearby Rydberg levels of opposite parity  $|\uparrow\rangle_i = |r\rangle_i$ ,  $|\downarrow\rangle_i = |r'\rangle_i$ . In this case, the dipolar interactions are described by an XY model with long-range  $1/R^3$  couplings, see Fig. 1. Below, we describe how to obtain the desired LGT by periodically driving the atoms, exploiting Floquet engineering [53] in a way that effectively gauges the global symmetry of the XY model, transforming it to a local  $\mathbb{Z}_2$  gauge symmetry, where some atoms represent matter, and some others gauge fields.

*Target model.* Our goal is to achieve the  $\mathbb{Z}_2$  LGT

$$H_{\mathbb{Z}_2} = \sum_{n=1}^N J_t (a_n^\dagger \tau_{n+\frac{1}{2}}^z a_{n+1} + \text{H.c.}) + \mu (-1)^n a_n^\dagger a_n + h \tau_{n+\frac{1}{2}}^x, \quad (1)$$

where  $J_t$  is the tunneling strength, and  $h$  ( $\mu$ ) plays the role of the electric-field coupling strength (particle mass). The matter content corresponds to hardcore bosons that can be created (annihilated)  $a_n^\dagger$  ( $a_n$ ) at the lattice sites, such that double occupancies are forbidden ( $(a_n^\dagger)^2 = (a_n)^2 = 0$ ). The gauge fields are described by magnetic-type (electric-type) Pauli operators  $\tau_{n+1/2}^z$  ( $\tau_{n+1/2}^x$ ) on the links, allowing for a local symmetry

$[H_{\mathbb{Z}_2}, G_n] = 0$ ,  $G_n = \tau_{n-1/2}^x \exp\{i\pi a_n^\dagger a_n\} \tau_{n+1/2}^x$ . As is customary, hardcore bosons can be mapped to fermions through a Jordan-Wigner transformation  $a_n = \prod_{m < n} e^{i\pi c_m^\dagger c_m} c_n$ , such that a further phase transformation  $c_n \rightarrow c_n e^{i\frac{\pi}{2}n}$  maps Eq. (1) onto the Kogut-Susskind  $\mathbb{Z}_2$  LGT on a chain [54,55].

*Nearest-neighbor Floquet scheme.* Before delving into the additional complexity of the dipolar Rydberg case, we illustrate our Floquet scheme for nearest-neighbor interactions. This case corresponds to the XY chain [56] with dynamical longitudinal  $h_i^z$  and transverse  $h_i^x$  fields

$$H_{XY} = \sum_{i=1}^{N_a} J (\sigma_i^+ \sigma_{i+1}^- + \text{H.c.}) + h_i^z \sigma_i^z + h_i^x \sigma_i^x, \quad (2)$$

where  $\sigma_i^\alpha$ ,  $\alpha = x, z, \pm$  are diagonal and ladder operators of the Pauli algebra, and we take  $\hbar = 1$  such that all couplings in (2) have units of Hz. Since we aim at generating three-body terms (1) from two-body interactions (2), second-order processes  $\mathcal{O}(J^2)$  should outweigh first-order ones  $\mathcal{O}(J)$ . Moreover, to achieve gauge invariance, the scheme should single out a specific set of terms from all possible second-order processes. We shall see that both of the above problems can be overcome through a selective driving protocol.

Specifically, we consider a Floquet scheme that drives the odd spins with a time-periodic longitudinal field of frequency  $\omega_d$ , strength  $\eta \omega_d$ , and phase  $\varphi_i$ , together with a static staggered part  $h_i^z = \frac{1}{2} [(-1)^i \delta h + \eta \omega_d \cos(\omega_d t + \varphi_i)] \delta_{i, \text{odd}}$ . The even spins are instead subject to a static transverse field  $h_i^x = \frac{\Omega}{2} \delta_{i, \text{even}}$ . To achieve the aforementioned selective dressing, we first need to inhibit the gauge-breaking first-order terms. For this, we exploit a spin-version of the coherent destruction of tunneling [57,58], through which  $\mathcal{O}(J)$  terms get dressed by the absorption/emission of energy packets  $\epsilon_\ell = \ell \omega_d$ ,  $\ell \in \mathbb{Z}$ , from/into the driving field. By using a very fast modulation  $\omega_d \gg J$ , these processes become off resonant, and the XY coupling gets dressed by the  $\ell = 0$  term as  $J \rightarrow J J_0(\eta)$ . Thus, by setting the relative amplitude to zero of this Bessel function, the first-order terms get suppressed.

At second order  $\mathcal{O}(J^2/\omega_d)$ , we get three types of processes: assisted tunnelings between odd sites  $\sigma_{2n-1}^+ \sigma_{2n}^z \sigma_{2n+1}^-$ , assisted tunnelings between even sites  $\sigma_{2n}^+ \sigma_{2n+1}^z \sigma_{2n+2}^-$ , and two-body terms arising from back and forth spin flips. The effective Hamiltonian reads

$$H_{\text{eff}} = \sum_{i \text{ even}} \frac{\Omega}{2} \sigma_i^x + \sum_{i \text{ odd}} (-1)^{\frac{i+1}{2}} \frac{\delta h}{2} \sigma_i^z + \sum_{\langle i, j, k \rangle} \frac{J^2}{\omega_d} \chi_{ik} \sigma_i^+ \sigma_j^z \sigma_k^-, \quad (3)$$

where  $\langle i, j, k \rangle$  is a nearest-neighbor triplet. Here, we have introduced a dressing parameter that contains all second-order processes where  $\ell$  “quanta” are virtually absorbed from and emitted into the driving field

$$\chi_{ik} = \sum_{\ell > 0} \frac{2i}{\ell} J_\ell^2(\eta) \sin[\ell(\varphi_k - \varphi_i)]. \quad (4)$$

We note that, in spite of the sum in Eq. (3) including all possible triplets,  $\chi_{ik}$  is nonzero only for  $i \neq k$  both odd, as all other cases “see” the same driving phase  $\varphi_i - \varphi_k = 0 \pmod{2\pi}$ . We thus achieve the desired selectivity by a de-

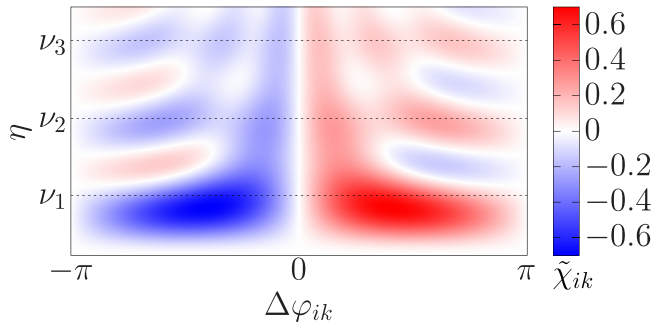


FIG. 2. Dressing parameter.  $\tilde{\chi}_{ik} = -i\chi_{ik}$  is depicted as a function of the phase difference  $\Delta\varphi_{ik}$  and relative driving strength  $\eta$ . Here  $\nu_n$  denotes the  $n$ th zero of  $J_0(x)$ . For  $\eta = \nu_1$ ,  $\tilde{\chi}_{ik}$  has a maximum (minimum) at  $\Delta\varphi_{ik} = 60^\circ$  ( $-60^\circ$ ).

structive interference, canceling all second-order processes but those with  $\varphi_i \neq \varphi_k$ . These processes correspond to the tunneling of an excitation between odd spins depending on the population of the intermediate even spin (see the Supplemental Material [59]). In order to maximize such assisted tunneling, it is convenient to choose  $\eta = \nu_1 \approx 2.405$  and  $\varphi_{2n+1} = n\frac{\pi}{3}$ , where  $\nu_1$  denotes the first zero of the Bessel function  $J_0(\eta)$  (see Fig. 2). With this choice  $\chi_{2n-1,2n+1} = \chi \approx -0.63i$ , the dressed second-order dynamics is slower by a factor of  $|J\chi/\omega_d| \approx 0.06$ . Equation (1) can be finally obtained by identifying matter (gauge fields) with the odd (even) spins, such that  $N_a = 2N + 1$ :  $a_n = \sigma_{2n+1}^-$ ,  $a_n^\dagger = \sigma_{2n+1}^+$ ,  $\tau_{n+1/2}^z = \sigma_{2n}^z$ ,  $\tau_{n+1/2}^x = \sigma_{2n}^x$ , together with the following parameters:

$$J_t = \frac{J^2}{\omega_d}\chi, \quad h = \frac{\Omega}{2}, \quad \mu = \delta h. \quad (5)$$

After presenting our Floquet QS scheme, we provide numerical benchmarks that support its validity. We consider an initial state that allows to discuss confinement. In the LGT language, such a state corresponds to a pair of dynamical charges at positions  $n_1$  and  $n_2$  connected by an electric-field string  $|\psi_0\rangle = |0, -\dots-, 1_{n_1}, +, 0, +\dots+, 1_{n_2}, -, 0, -\dots-, 0\rangle$ , where  $\tau^x|\pm\rangle = \pm|\pm\rangle$ . This initial state belongs to the neutral gauge sector  $G_n|\psi_0\rangle = |\psi_0\rangle \forall n \neq 1, N$ . We consider the case  $\Omega \neq 0$ ,  $\delta h = 0$ , and simulate the real-time dynamics of the periodically modulated XY chain (2) of  $2N + 1 = 21$  spins using matrix-product-state algorithms (TEDB) [60–63]. In Fig. 3, we display the obtained time evolution: indeed, the charges do not spread indefinitely but instead perform periodic oscillations around their initial positions, accompanied by the stretching and compressing of the electric string. Indeed, when  $\Omega \neq 0$ , the effective  $\mathbb{Z}_2$  model (1) is characterized by a nonzero electric coupling  $h = \frac{\Omega}{2}$ . In this case, pairs of particles separated by a positive electric string experience an attracting potential that grows linearly with the string length, and are confined into mesonlike bound states [25,64]. The relative coordinate wave-function solves a Wannier-Stark equation, and thus Bloch oscillations arise [40,64,65]. The observed dynamics is effectively restricted to the neutral gauge sector, in agreement with Eq. (1), within errors which come from higher-order Floquet terms. The amount of

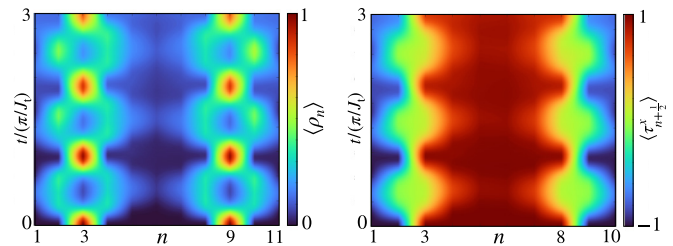


FIG. 3.  $\mathbb{Z}_2$  confinement. Two particles are initialized at positions  $i = 3, 9$  and connected by an electric-field string. Here,  $h = J_t$  and  $\mu = 0$ . Left and right panels correspond to the contour plots of the charge distribution  $\langle \rho_n(t) \rangle = \langle \psi(t) | a_n^\dagger a_n | \psi(t) \rangle$  and the electric field  $\langle \tau_{n+1/2}^x(t) \rangle$ , where the evolution of  $|\psi(t)\rangle$  under  $H_{XY}(t)$  with  $\omega_d = 30J$  is approximated using MPS with bond dimension = 20.

gauge-breaking grows with time, but remains below 15% violation of the condition  $G_n|\psi_0\rangle = |\psi_0\rangle \forall n \neq 1, N$ —see the Supplemental Material [59].

*Dipolar Floquet-Rydberg scheme.* After presenting the ideal nearest-neighbor Floquet scheme, we provide details for the implementation through Rydberg-atom arrays [51,52]. We note that the Rydberg levels  $|r\rangle$  and  $|r'\rangle$  we refer to are  $r = nL_J, m$  and  $r' = n'L'_J, m'$ , having opposite parity and dipole-allowed transitions, e.g.,  $L = S$  or  $P$  and  $L' = P$  or  $D$  with  $\Delta J, \Delta m \in \{0, \pm 1\}$ . In this case, the leading dipolar interactions [66,67] encompass pairwise excitation-transfer  $(r_i, r_j) = (r, r') \leftrightarrow (r', r)$  even for a vanishing electric field [68–73]. This energy transfer can be described by a dipolar version  $H_{XY}^{\text{dip}}$  of the XY model (2), with  $J \mapsto J_{ij}$ . The couplings  $J_{ij}$  display an angular dependence  $J_{ij} = J_3(3 \cos^2 \theta_{ij} - 1)/R_{ij}^3$ , where  $\theta_{ij}$  is the angle between the interatomic vector  $\mathbf{R}_{ij}$  and an external magnetic field  $\mathbf{B}_0$  (fixing the atoms quantization axis) [70,71,74,75]. For instance,  $|J_{ij}|/2\pi \sim 1\text{--}10$  MHz for  $^{87}\text{Rb}$  atoms with  $n, n' \sim 50\text{--}60$  at  $R_{ij} \sim 10\text{--}15 \mu\text{m}$  distances, which exceed the linewidths set by the Rydberg lifetimes even at room temperatures  $T_1 \sim 100\text{--}200 \mu\text{s}$  [76].

In principle, the long-range terms could lead to additional gauge-violating processes. Therefore, we selectively address even-even/odd-odd and odd-even interactions. We can suppress the even-even/odd-odd processes by taking the magnetic field  $\mathbf{B}_0$  along a specific direction relative to the Rydberg array. For  $\mathbf{B}_0 \parallel \mathbf{R}_{ij}$  ( $\mathbf{B}_0 \perp \mathbf{R}_{ij}$ ), the interactions are antiferromagnetic  $J_{ij} > 0$  [70,72] (ferromagnetic  $J_{ij} < 0$  [73]). As exploited in [75], when  $\mathbf{B}_0$  is directed along the plane containing a Rydberg ladder, the XY couplings between distant spins making an angle  $\theta_{ij} = \theta_m := 54.7^\circ$  vanish, yielding approximately a dimerized XY model.

In our context, this arrangement would suppress the gauge-violating processes involving even-even (odd-odd) spins. On the other hand, the dimerization would activate higher-order terms in the high-frequency Floquet expansion, limiting the timescale of validity of the QS (see the Supplemental Material [59]). To overcome this problem, we propose to lift the quantising field such that  $\mathbf{B}_0$  is out of plane at an angle  $\theta_m$  with the normal vector to the Rydberg ladder (here corresponding to the  $z$  axis)—see Fig. 1. With this choice, besides suppressing the undesired even-even (odd-odd) couplings, the

higher-order Floquet terms due to the dimerization do not contribute. Defining  $\phi_{ij}$  as the angle that  $\mathbf{R}_{ij}$  makes with the projection of the quantizing field into the Rydberg array  $\mathbf{B}_0^\perp$ , we find that  $J_{ij} = J_3(2 \cos^2 \phi_{ij} - 1)$ . Therefore, when  $\phi_{ij} = \phi_m := 45^\circ$ , the atoms on the upper (bottom) leg of the ladder correspond to the vertices of isosceles right triangles, whose sides have length  $d$  and whose base has length  $b = \sqrt{2}d$ , which lies along the legs of the ladder. This choice results in  $J_{ij} = 0$  for pairs of atoms within the same leg, which correspond to the undesired even-even (odd-odd) spin couplings. The expression for the nonzero XY couplings is

$$J_{ij} = -\frac{J_3 r}{d^3} \left( \frac{2}{1+r^2} \right)^{5/2}, \quad r = i - j, \quad (6)$$

where the indices  $i$  and  $j$  must be odd and even, respectively (see the Supplemental Material [59]). We thus see that  $|J_{i,i\pm 1}| = J_3/d^3$ , such that there is no dimerization, and no higher-order gauge-breaking terms in the Floquet scheme associated to it. Additionally, the couplings  $|i - j| > 1$  are highly suppressed by the dipolar law.

Following the same driving protocol as for the nearest-neighbor Floquet scheme, we obtain the effective Hamiltonian

$$H_{\text{eff}} = \sum_{i,j,k=1}^{N_a} \frac{J_{ij} J_{jk}}{\omega_d} \chi_{ik} \sigma_i^+ \sigma_j^z \sigma_k^-, \quad (7)$$

where the long-range nature of the XY couplings sets an assisted tunneling involving generic spin triplets [not necessarily nearest-neighbors as in the scheme adopted for (3)]. We note that the dressing parameter  $\chi_{ik}$  is still given by Eq. (4), and we can again exploit the destructive-interference selectivity, such that the tunneling only occurs between odd spins  $i \neq k$  mediated by an even spin at  $j$ . However, there are additional longer-range terms of this form that would break the gauge symmetry, the largest being  $\sigma_{2n-1}^+ \sigma_{2n}^z \sigma_{2n+3}^-$  and  $\sigma_{2n-1}^+ \sigma_{2n+2}^z \sigma_{2n+1}^-$ . We get rid of the former by appropriately choosing the driving phases according to  $\varphi_{2n+1} = n\frac{\pi}{2}$  [see Eq. (6)], while the latter are much smaller  $J_{1,4}/J_{1,2} \approx 0.05$ , which follows from Eq. (6). By sticking to the previous choice for the driving amplitude  $\eta = \nu_1$ , we find that  $\chi_{2n-1,2n+1} = \chi \approx -0.5i$ . One can use the effective tunneling in Eq. (5), and map the Floquet-Rydberg QS to the target  $\mathbb{Z}_2$  LGT as before.

As done for the n.n. model, now we benchmark our scheme by comparing the Floquet effective dynamics with the time-evolution of the original Rydberg system. Due to the long-range nature of the microscopic model, we resort to exact numerical methods, limiting the system sizes up to  $N_a = 9$  spins. We consider the initial state with a single charge  $|\psi_0\rangle = |1_1, -, 0, -\dots, 0\rangle$ , and calculate numerically the time-evolution operator by a Trotter expansion within one period of the drive  $U_T = \prod_i e^{-iH_{\text{XY}}^{\text{dip}}(t_i)\delta t}$ , where we have taken  $\delta t = T/410$  to minimize the numerical errors. The stroboscopic dynamics is obtained as  $|\psi(nT)\rangle = U_T^n |\psi_0\rangle$ , with  $n \in \mathbb{N}$ . The results are compared with the effective gauge-invariant dynamics of Eq. (1), which have an exact solution in terms of a Wannier-Stark ladder in the single-charge sector. In the case of two matter sites and a single link, we find that the large-frequency  $\omega_d \gg J$  regime perfectly realizes the expected gauge-invariant evolution (see Fig. 4). Indeed, the dynam-

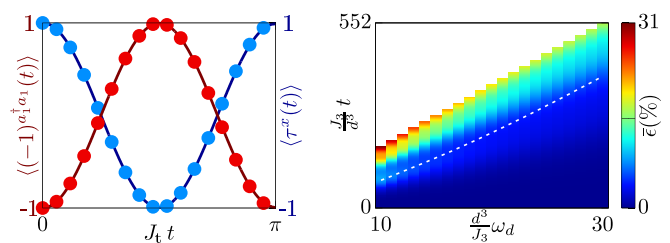


FIG. 4. *Gauge-invariant dynamics and gauge violation.* The left panel displays the driven dynamics (solid line) and the effective gauge-invariant dynamics (dots) arising from the initial state  $|L\rangle = |1, -, 0\rangle$ , in the  $N_a = 3$ ,  $\omega_d = 30J_3/d^3$  case. The driven evolution is in full-agreement with the expected periodic oscillations of  $\langle a_n^\dagger(t) \rangle$ ,  $\langle \tau^x(t) \rangle$ . The right panel corresponds to the average percent error  $\bar{\epsilon}(t, \omega_d)$  accumulated during the evolution from the state  $|\psi_0\rangle = |1_1, -, 0, -\dots, 0\rangle$ , in the case  $N_a = 9$ . For each value of the driving frequency  $\omega_d$ , only times up to  $3\pi/J_1(\omega_d)$  are explored. The dashed line corresponds to a 10% threshold of gauge violation.

ics is restricted to the subspace spanned by  $|L\rangle = |1, -, 0\rangle$  and  $|R\rangle = |0, +, 1\rangle$ , which are gauge-invariant according to  $G_n = (-1)^{a_n} \tau^x$ , with local charges  $q_n = (-1)^n$ . The tunneling dynamics leads to Rabi oscillations between  $|L\rangle/|R\rangle$ , provided that the electric field is periodically switched on/off  $|+\rangle/|-\rangle$  to comply with gauge invariance. As figures of merit, we display the real-time evolution of the  $\mathbb{Z}_2$  charge  $\langle (-1)^{a_n^\dagger} \rangle$ , and the electric field  $\langle \tau^x \rangle$ .

The agreement with the  $\mathbb{Z}_2$  gauge-invariant dynamics can be affected by two main sources of error. The first corresponds to gauge-breaking processes that arise from the higher orders in the large-frequency Floquet expansion. The second derives from the long-range XY couplings. To estimate the amount of gauge violation, we extend our simulations to the case of nine spins, and allow to sweep the driving frequency. We evaluate the average percent error  $\bar{\epsilon}(t, \omega_d) = \frac{100}{N_a} \sum_n |\frac{G_n(t, \omega_d) - q_n}{q_n}|$ . As shown in Fig. 4, the amount of gauge violation is below a 10% threshold for values of  $\frac{J_3}{d^3} t$  that are compatible with currently achieved experimental times. We note that, as  $\omega_d$  is increased, the agreement between driven and effective dynamics grows, as a result of the  $(1/\omega_d)^\ell$  suppression of  $(\ell + 1)$ th order terms in the high-frequency expansion. To further stabilize the agreement to the gauge-invariant dynamics over longer time scales, one could resort to gauge-protection schemes to penalize gauge-violating processes [77,78].

So far, we have focused on the gauge-invariant tunneling stemming from  $H_{\text{eff}}$  (7). The required longitudinal  $\sum_{i \text{ even}} \frac{\Omega}{2} \sigma_i^x$  and transverse  $\sum_{i \text{ odd}} (-1)^{\frac{i+1}{2}} \frac{\delta h}{2} \sigma_i^z$  fields, as well as the time-periodic modulation, require local addressing in the Rydberg platform. This can be achieved by using laser beams suitably diffracted using acousto-optic deflectors. The lasers addressed to the even atoms should drive Raman transitions with a two-photon Rabi frequency  $\Omega$  that is resonant with the two Rydberg energy levels  $\omega_{L,1} - \omega_{L,2} = \omega_0$ , e.g., [79]. For the odd atoms, on the other hand, a pair of counterpropagating laser beams far off resonant  $\tilde{\omega}_{L,1} - \tilde{\omega}_{L,2} =: \omega_d \ll \omega_0$ , lead to differential ac-Stark shifts with contributions stemming from each of the laser beams, which have been previously used to induce a local constant longitudinal field in a two-atom XY model [72]. For our purposes, these local

ac-Stark shifts must be tuned to account for the staggering  $\delta h$ . Since we consider a pair of laser beams, there is also a traveling standing-wave pattern coming from their interference, which can be exploited for the time-periodic longitudinal field. The amplitude of this modulation  $\eta\omega_d$  is controlled by the crossed-beam two-photon Rabi frequencies, whereas the phase depends on the wave vectors  $\varphi_i = (\mathbf{k}_{L,1} - \mathbf{k}_{L,2}) \cdot \mathbf{R}_i$ . These laser-induced terms can be of the same order as the XY couplings, which requires using high-power lasers to allow for large detunings from other excited states, such that  $\delta h, \Omega, \eta\omega_d \sim 0.1\text{--}10$  MHz. We note that, while local addressing single atoms can in general introduce decay channels, resulting in an effective reduction of the lifetime of the Rydberg states, such effect would be negligibly small within the required range of parameters [72].

*Conclusions and outlook.* We have devised a protocol for the analog quantum simulation of a  $\mathbb{Z}_2$ LGT through Floquet engineering, and shown that it can be realized with Rydberg atoms trapped in optical tweezers. The proposed protocol generates specific gauge-invariant three-body terms (1) from two-body gauge-breaking couplings (2) by exploiting a selective dressing that makes use of time-periodic Floquet

modulation and a destructive interference that depends on the relative inhomogeneous phase of the modulation. The strong dipole-dipole interactions in Rydberg atoms make them ideally suited to realize this gauge-invariant dressing, as the weaker second-order processes in Eq. (5) can still be faster than typical decay times. On the other hand, we note that our scheme can be directly translated to trapped-ion or superconducting-qubit platforms, in which effective XY models have also been demonstrated. Provided that leading noise sources are minimized further, our proposal for a  $\mathbb{Z}_2$ LGT QS could also work there.

*Acknowledgments.* We thank P. Castorina, P. Kitson, G. Marchegiani, P. Naldesi, F. Percivalle, and J. Polo for discussions. A.B. acknowledges support from PID2021-127726NB-I00 (MCIU/AEI/FEDER, UE), from the Grant IFT Centro de Excelencia Severo Ochoa CEX2020-001007-S, funded by MCIN/AEI/10.13039/501100011033, from the CSIC Research Platform on Quantum Technologies PTI-001, from the MINECO through the QUANTUM ENIA project call - QUANTUM SPAIN project, and from the EU through the RTRP-NextGenerationEU within the framework of the Digital Spain 2025 Agenda.

- 
- [1] M. E. Peskin and D. V. Schroeder, *An Introduction to Quantum Field Theory* (Addison-Wesley, Reading, USA, 1995).
- [2] C. N. Yang and R. L. Mills, Conservation of isotopic spin and isotopic gauge invariance, *Phys. Rev.* **96**, 191 (1954).
- [3] K. G. Wilson, Confinement of quarks, *Phys. Rev. D* **10**, 2445 (1974).
- [4] J. Greensite, *Introduction to the Confinement Problem* (Springer Nature, Switzerland, 2020).
- [5] S. Durr, Z. Fodor, J. Frison, C. Hoelbling, R. Hoffmann, S. D. Katz, S. Krieg, T. Kurth, L. Lellouch, T. Lippert, K. K. Szabo, and G. Vulvert, *Ab initio* determination of light hadron masses, *Science* **322**, 1224 (2008).
- [6] K. Nagata, Finite-density lattice QCD and sign problem: Current status and open problems, *Prog. Part. Nucl. Phys.* **127**, 103991 (2022).
- [7] R. P. Feynman, Simulating physics with computers, *Int. J. Theor. Phys.* **21**, 467 (1982).
- [8] J. I. Cirac and P. Zoller, Goals and opportunities in quantum simulation, *Nat. Phys.* **8**, 264 (2012).
- [9] M. A. Nielsen and I. L. Chuang, *Quantum Computation and Quantum Information* (Cambridge University Press, 2000).
- [10] U.-J. Wiese, Ultracold quantum gases and lattice systems: quantum simulation of lattice gauge theories, *Ann. Phys.* **525**, 777 (2013).
- [11] E. Zohar, J. I. Cirac, and B. Reznik, Quantum simulations of lattice gauge theories using ultracold atoms in optical lattices, *Rep. Prog. Phys.* **79**, 014401 (2016).
- [12] M. Dalmonte and S. Montangero, Lattice gauge theory simulations in the quantum information era, *Contemp. Phys.* **57**, 388 (2016).
- [13] M. C. Bañuls, R. Blatt, J. Catani, A. Celi, J. I. Cirac, M. Dalmonte, L. Fallani, K. Jansen, M. Lewenstein, S. Montangero, C. A. Muschik, B. Reznik, E. Rico, L. Tagliacozzo, K. Van Acoleyen, F. Verstraete, U.-J. Wiese, M. Wingate, J. Zakrzewski, and P. Zoller, Simulating lattice gauge theories within quantum technologies, *Eur. Phys. J. D* **74**, 165 (2020).
- [14] M. C. Bañuls and K. Cichy, Review on novel methods for lattice gauge theories, *Rep. Prog. Phys.* **83**, 024401 (2020).
- [15] M. Aidelsburger, L. Barbiero, A. Bermudez, T. Chanda, A. Dauphin, D. González-Cuadra, P. R. Grzybowski, S. Hands, F. Jendrzejewski, J. Jünemann, G. Juzeliūnas, V. Kasper, A. Piga, S.-J. Ran, M. Rizzi, G. Sierra, L. Tagliacozzo, E. Tirrito, T. V. Zache, J. Zakrzewski *et al.*, Cold atoms meet lattice gauge theory, *Philos. Trans. R. Soc. A* **380**, 20210064 (2022).
- [16] N. Klco, A. Roggero, and M. J. Savage, Standard model physics and the digital quantum revolution: thoughts about the interface, *Rep. Prog. Phys.* **85**, 064301 (2022).
- [17] C. W. Bauer, Z. Davoudi, A. B. Balantekin, T. Bhattacharya, M. Carena, W. A. de Jong, P. Draper, A. El-Khadra, N. Gemelke, M. Hanada, D. Kharzeev, H. Lamm, Y.-Y. Li, J. Liu, M. Lukin, Y. Meurice, C. Monroe, B. Nachman, G. Pagano, J. Preskill *et al.*, Quantum simulation for high-energy physics, *PRX Quantum* **4**, 027001 (2023).
- [18] S. Flannigan, N. Pearson, G. H. Low, A. Buyskikh, I. Bloch, P. Zoller, M. Troyer, and A. J. Daley, Propagation of errors and quantitative quantum simulation with quantum advantage, *Quantum Sci. Technol.* **7**, 045025 (2022).
- [19] R. Trivedi, A. F. Rubio, and J. I. Cirac, Quantum advantage and stability to errors in analogue quantum simulators, [arXiv:2212.04924](https://arxiv.org/abs/2212.04924).
- [20] J. Schwinger, Gauge invariance and mass. II, *Phys. Rev.* **128**, 2425 (1962).
- [21] S. Coleman, R. Jackiw, and L. Susskind, Charge shielding and quark confinement in the massive schwinger model, *Ann. Phys.* **93**, 267 (1975).
- [22] G. 't Hooft, A two-dimensional model for mesons, *Nucl. Phys. B* **75**, 461 (1974).

- [23] D. J. Gross and W. Taylor, Two-dimensional QCD is a string theory, *Nucl. Phys. B* **400**, 181 (1993).
- [24] F. J. Wegner, Duality in generalized ising models and phase transitions without local order parameters, *J. Math. Phys.* **12**, 2259 (1971).
- [25] U. Borla, R. Verresen, F. Grusdt, and S. Moroz, Confined phases of one-dimensional spinless fermions coupled to  $\mathbb{Z}_2$  gauge theory, *Phys. Rev. Lett.* **124**, 120503 (2020).
- [26] M. c. v. Kębrič, L. Barbiero, C. Reinmoser, U. Schollwöck, and F. Grusdt, Confinement and mott transitions of dynamical charges in one-dimensional lattice gauge theories, *Phys. Rev. Lett.* **127**, 167203 (2021).
- [27] D. González-Cuadra, L. Tagliacozzo, M. Lewenstein, and A. Bermudez, Robust topological order in fermionic  $\mathbb{Z}_2$  gauge theories: From Aharonov-Bohm instability to soliton-induced deconfinement, *Phys. Rev. X* **10**, 041007 (2020).
- [28] J. Nyhegn, C.-M. Chung, and M. Burrello,  $\mathbb{Z}_N$  lattice gauge theory in a ladder geometry, *Phys. Rev. Res.* **3**, 013133 (2021).
- [29] A. Kitaev, Fault-tolerant quantum computation by anyons, *Ann. Phys.* **303**, 2 (2003).
- [30] X.-G. Wen, Topological order: From long-range entangled quantum matter to a unified origin of light and electrons, *ISRN Condens. Matter Phys.* **2013**, 1 (2013).
- [31] E. Fradkin and S. H. Shenker, Phase diagrams of lattice gauge theories with Higgs fields, *Phys. Rev. D* **19**, 3682 (1979).
- [32] I. S. Tupitsyn, A. Kitaev, N. V. Prokof'ev, and P. C. E. Stamp, Topological multicritical point in the phase diagram of the toric code model and three-dimensional lattice gauge Higgs model, *Phys. Rev. B* **82**, 085114 (2010).
- [33] S. Gazit, M. Randeria, and A. Vishwanath, Emergent dirac fermions and broken symmetries in confined and deconfined phases of  $\mathbb{Z}_2$  gauge theories, *Nat. Phys.* **13**, 484 (2017).
- [34] S. Gazit, F. F. Assaad, S. Sachdev, A. Vishwanath, and C. Wang, Confinement transition of  $\mathbb{Z}_2$  gauge theories coupled to massless fermions: Emergent quantum chromodynamics and  $SO(5)$  symmetry, *Proc. Natl. Acad. Sci. USA* **115**, E6987 (2018).
- [35] C. Muschik, M. Heyl, E. Martinez, T. Monz, P. Schindler, B. Vogell, M. Dalmonte, P. Hauke, R. Blatt, and P. Zoller, U(1) Wilson lattice gauge theories in digital quantum simulators, *New J. Phys.* **19**, 103020 (2017).
- [36] Z. Davoudi, M. Hafezi, C. Monroe, G. Pagano, A. Seif, and A. Shaw, Towards analog quantum simulations of lattice gauge theories with trapped ions, *Phys. Rev. Res.* **2**, 023015 (2020).
- [37] G. Pardo, T. Greenberg, A. Fortinsky, N. Katz, and E. Zohar, Resource-efficient quantum simulation of lattice gauge theories in arbitrary dimensions: Solving for Gauss's law and fermion elimination, *Phys. Rev. Res.* **5**, 023077 (2023).
- [38] R. Irmejs, M.-C. Bañuls, and J. I. Cirac, Quantum simulation of  $\mathbb{Z}_2$  lattice gauge theory with minimal resources, *Phys. Rev. D* **108**, 074503 (2023).
- [39] L. Barbiero, C. Schweizer, M. Aidelsburger, E. Demler, N. Goldman, and F. Grusdt, Coupling ultracold matter to dynamical gauge fields in optical lattices: From flux attachment to  $\mathbb{Z}_2$  lattice gauge theories, *Sci. Adv.* **5**, eaav7444 (2019).
- [40] O. Băzăvan, S. Saner, E. Tirrito, G. Araneda, R. Srinivas, and A. Bermudez, Synthetic  $\mathbb{Z}_2$  gauge theories based on parametric excitations of trapped ions, [arXiv:2305.08700](https://arxiv.org/abs/2305.08700).
- [41] J. Zhang, J. Unmuth-Yockey, J. Zeiher, A. Bazavov, S.-W. Tsai, and Y. Meurice, Quantum simulation of the universal features of the polyakov loop, *Phys. Rev. Lett.* **121**, 223201 (2018).
- [42] S. Notarnicola, M. Collura, and S. Montangero, Real-time-dynamics quantum simulation of (1 + 1)-dimensional lattice qed with Rydberg atoms, *Phys. Rev. Res.* **2**, 013288 (2020).
- [43] A. Celi, B. Vermersch, O. Viyuela, H. Pichler, M. D. Lukin, and P. Zoller, Emerging two-dimensional gauge theories in Rydberg configurable arrays, *Phys. Rev. X* **10**, 021057 (2020).
- [44] D. González-Cuadra, T. V. Zache, J. Carrasco, B. Kraus, and P. Zoller, Hardware efficient quantum simulation of non-Abelian gauge theories with qudits on Rydberg platforms, *Phys. Rev. Lett.* **129**, 160501 (2022).
- [45] S. Ohler, M. Kiefer-Emmanouilidis, A. Browaeys, H. P. Büchler, and M. Fleischhauer, Self-generated quantum gauge fields in arrays of Rydberg atoms, *New J. Phys.* **24**, 023017 (2022).
- [46] J. Mildenerger, W. Mruczkiewicz, J. C. Halimeh, Z. Jiang, and P. Hauke, Probing confinement in a  $\mathbb{Z}_2$  lattice gauge theory on a quantum computer, [arXiv:2203.08905](https://arxiv.org/abs/2203.08905).
- [47] L. Homeier, A. Bohrdt, S. Linsel, E. Demler, J. C. Halimeh, and F. Grusdt, Realistic scheme for quantum simulation of  $\mathbb{Z}_2$  lattice gauge theories with dynamical matter in  $(2 + 1)d$ , *Commun. Phys.* **6**, 127 (2023).
- [48] D. González-Cuadra, D. Bluvstein, M. Kalinowski, R. Kaubruegger, N. Maskara, P. Naldesi, T. V. Zache, A. M. Kaufman, M. D. Lukin, H. Pichler, B. Vermersch, J. Ye, and P. Zoller, Fermionic quantum processing with programmable neutral atom arrays, *Proc. Natl. Acad. Sci. USA* **120**, e2304294120 (2023).
- [49] C. Schweizer, F. Grusdt, M. Berngruber, L. Barbiero, E. Demler, N. Goldman, I. Bloch, and M. Aidelsburger, Floquet approach to  $\mathbb{Z}_2$  lattice gauge theories with ultracold atoms in optical lattices, *Nat. Phys.* **15**, 1168 (2019).
- [50] H. C. J. Gan, G. Maslennikov, K.-W. Tseng, C. Nguyen, and D. Matsukevich, Hybrid quantum computing with conditional beam splitter gate in trapped ion system, *Phys. Rev. Lett.* **124**, 170502 (2020).
- [51] A. Browaeys, D. Barredo, and T. Lahaye, Experimental investigations of dipole-dipole interactions between a few Rydberg atoms, *J. Phys. B: At., Mol. Opt. Phys.* **49**, 152001 (2016).
- [52] M. Morgado and S. Whitlock, Quantum simulation and computing with Rydberg-interacting qubits, *AVS Quantum Science* **3**, 023501 (2021).
- [53] A. Eckardt, *Colloquium: Atomic quantum gases in periodically driven optical lattices*, *Rev. Mod. Phys.* **89**, 011004 (2017).
- [54] J. Kogut and L. Susskind, Hamiltonian formulation of Wilson's lattice gauge theories, *Phys. Rev. D* **11**, 395 (1975).
- [55] L. Susskind, Lattice fermions, *Phys. Rev. D* **16**, 3031 (1977).
- [56] E. Lieb, T. Schultz, and D. Mattis, Two soluble models of an antiferromagnetic chain, *Ann. Phys.* **16**, 407 (1961).
- [57] D. H. Dunlap and V. M. Kenkre, Dynamic localization of a charged particle moving under the influence of an electric field, *Phys. Rev. B* **34**, 3625 (1986).
- [58] H. Lignier, C. Sias, D. Ciampini, Y. Singh, A. Zenesini, O. Morsch, and E. Arimondo, Dynamical control of matter-wave tunneling in periodic potentials, *Phys. Rev. Lett.* **99**, 220403 (2007).
- [59] See Supplemental Material at <http://link.aps.org/supplemental/10.1103/PhysRevResearch.6.L022059> for the derivation of the target  $\mathbb{Z}_2$  LGT at second order in the Floquet perturbative analysis. Key points for the experimental realization of the proposed

- Floquet scheme are also discussed and additional details are provided about the impact of gauge-violating processes.
- [60] M. Fishman, S. R. White, and E. M. Stoudenmire, The ITensor software library for Tensor network calculations, *SciPost Phys. Codebases*, **4** (2022).
- [61] M. Fishman, S. R. White, and E. M. Stoudenmire, Codebase release 0.3 for ITensor, *SciPost Phys. Codebases*, **4** (2022).
- [62] D. Perez-Garcia, F. Verstraete, M. M. Wolf, and J. I. Cirac, Matrix product state representations, *Quantum Information & Computation* **7**, 401 (2007).
- [63] M. C. Bañuls, Tensor network algorithms: A route map, *Annu. Rev. Condens. Matter Phys.* **14**, 173 (2023).
- [64] F. M. Surace and A. Lerose, Scattering of mesons in quantum simulators, *New J. Phys.* **23**, 062001 (2021).
- [65] E. C. Domanti, P. Castorina, D. Zappalà, and L. Amico, Aharonov-Bohm effect for confined matter in lattice gauge theories, *Phys. Rev. Res.* **6**, 013268 (2024).
- [66] M. R. Flannery, D. Vrinceanu, and V. N. Ostrovsky, Long-range interaction between polar Rydberg atoms, *J. Phys. B: At., Mol. Opt. Phys.* **38**, S279 (2005).
- [67] S. Weber, C. Tresp, H. Menke, A. Urvoy, O. Firstenberg, H. P. Büchler, and S. Hofferberth, Calculation of Rydberg interaction potentials, *J. Phys. B: At., Mol. Opt. Phys.* **50**, 133001 (2017).
- [68] S. Bettelli, D. Maxwell, T. Fernholz, C. S. Adams, I. Lesanovsky, and C. Ates, Exciton dynamics in emergent Rydberg lattices, *Phys. Rev. A* **88**, 043436 (2013).
- [69] D. Maxwell, D. J. Szwer, D. Paredes-Barato, H. Busche, J. D. Pritchard, A. Gauguier, K. J. Weatherill, M. P. A. Jones, and C. S. Adams, Storage and control of optical photons using Rydberg polaritons, *Phys. Rev. Lett.* **110**, 103001 (2013).
- [70] D. Barredo, H. Labuhn, S. Ravets, T. Lahaye, A. Browaeys, and C. S. Adams, Coherent excitation transfer in a spin chain of three Rydberg atoms, *Phys. Rev. Lett.* **114**, 113002 (2015).
- [71] A. P. Orioli, A. Signoles, H. Wildhagen, G. Günter, J. Berges, S. Whitlock, and M. Weidemüller, Relaxation of an isolated dipolar-interacting Rydberg quantum spin system, *Phys. Rev. Lett.* **120**, 063601 (2018).
- [72] S. de Léséleuc, D. Barredo, V. Lienhard, A. Browaeys, and T. Lahaye, Optical control of the resonant dipole-dipole interaction between Rydberg atoms, *Phys. Rev. Lett.* **119**, 053202 (2017).
- [73] C. Chen, G. Emperauger, G. Bornet, F. Caleca, B. Gély, M. Bintz, S. Chatterjee, V. Liu, D. Barredo, N. Y. Yao, T. Lahaye, F. Mezzacapo, T. Roscilde, and A. Browaeys, Spectroscopy of elementary excitations from quench dynamics in a dipolar XY Rydberg simulator, [arXiv:2311.11726](https://arxiv.org/abs/2311.11726).
- [74] J. S. Frasier, Resonant processes in a frozen gas, [arXiv:cond-mat/0104551](https://arxiv.org/abs/cond-mat/0104551).
- [75] S. de Léséleuc, V. Lienhard, P. Scholl, D. Barredo, S. Weber, N. Lang, H. P. Büchler, T. Lahaye, and A. Browaeys, Observation of a symmetry-protected topological phase of interacting bosons with Rydberg atoms, *Science* **365**, 775 (2019).
- [76] M. Saffman and T. G. Walker, Analysis of a quantum logic device based on dipole-dipole interactions of optically trapped Rydberg atoms, *Phys. Rev. A* **72**, 022347 (2005).
- [77] J. C. Halimeh, H. Lang, J. Mildemberger, Z. Jiang, and P. Hauke, Gauge-symmetry protection using single-body terms, *PRX Quantum* **2**, 040311 (2021).
- [78] J. C. Halimeh, L. Homeier, C. Schweizer, M. Aidelsburger, P. Hauke, and F. Grusdt, Stabilizing lattice gauge theories through simplified local pseudogenerators, *Phys. Rev. Res.* **4**, 033120 (2022).
- [79] T. M. Graham, M. Kwon, B. Grinkemeyer, Z. Marra, X. Jiang, M. T. Lichtman, Y. Sun, M. Ebert, and M. Saffman, Rydberg-mediated entanglement in a two-dimensional neutral atom qubit array, *Phys. Rev. Lett.* **123**, 230501 (2019).